ELSEVIER

Ceramics International 33 (2007) 333–336

CERAMICS INTERNATIONAL

www.elsevier.com/locate/ceramint

Thick alumina dielectric films on aluminum through chemically bonded composite sol–gel

Hyungkeun Kim, Tom Troczynski *

Department of Materials Engineering, The University of British Columbia, 309-6350 Stores Road, Vancouver, BC, Canada V6T 1Z4

Received 3 August 2005; received in revised form 24 August 2005; accepted 22 September 2005
Available online 18 January 2006

Abstract

A new process for ~200 μm thick multilayer dielectric films on aluminum was developed via chemically bonded composite sol–gel. The sol–gel process used alumina and chemical bonding used phosphoric acid and aluminum phosphates. An interlayer was introduced between the coatings and aluminum substrate to decrease the thermal expansion mismatch between the ceramic and the substrate. The dielectric breakdown voltage of about 2500 V was measured for the films at room temperature.

Keywords: A. Sol–gel process; C. Dielectric properties; C. Thermal expansion; D. Al_2O_3

1. Introduction and background

Sol–gel (SG) technology is used to manufacture high quality glasses, fine ceramics, and electrical insulators, as it is relatively low temperature process delivering high purity of the final products [1–4]. In order to avoid high shrinkage during SG processing, calcined ceramic powders were dispersed into the sol to make composite sol–gel (CSG) [5–7]. The CSG allows deposition of about 20 μm thick, crack-free thick coatings. One of the biggest advantages of the composite sol–gel technology is to build up thick coatings, in some cases up to several mm. The chemically bonded composite sol–gel (CB-CSG) has been developed to further decrease the coating processing temperature, e.g. to 300 °C [8]. The CB-CSG uses a chemical reaction between alumina sol and phosphoric acid and forms a mono-aluminum phosphate ($Al(H_2PO_4)_3$).

This work has been motivated by the need for a simple process for deposition of ceramic films for electrical insulation, in particular to electrically insulate heating elements attached to a metal base, while minimizing the heat loss. The commercially available heating elements typically consist of a silver film resistor separated by a glass film from the base metal, such as stainless steel. Recently, we observed renewed interest in aluminum as the base metal for the heaters due to its lower density of ~2.7 g/cm^3, and higher thermal conductivity ~230 W/m K than the steel. At the same time, the possibilities of heat treatment of the aluminum alloy substrates during coating processing are severely limited. This triggered the need for new, lower temperature process for ceramic insulators and insulating coatings. CSG Silica (SiO_2) has received some attention, but its relatively low thermal conductivity (~1.4 W/m K) compared with that of alumina (~30 W/m K) degrades the performance of heating elements [9]. Olding et al. [5] fabricated ~100 μm thick alumina–silica films on stainless steel using CSG technology.

In this paper, the process development for predominantly alumina dielectric films on aluminum carried out by CB-CSG technology is presented. Relatively dense and thick (>200 μm) coatings are required for the ac breakdown voltage of at least 2000 V. In order to overcome the problem of the large thermal expansion mismatch between the (predominantly) alumina and the aluminum substrate, a porous (compliant) ceramic interlayer at the interface was introduced. Mixtures of different alumina particle sizes were investigated to modify the coating microstructure. The resulting microstructures, breakdown voltage, and thermal cycling properties were investigated, as a function of the process parameters.

2. Experimental procedures

Boehmite (AlOOH, <20 nm, SOL-2PK, Condea, Germany) was used for the alumina sol precursor, and two grades of

* Corresponding author. Tel.: +1 604 822 2612; fax: +1 604 822 3619.
E-mail address: troczyns@interchange.ubc.ca (T. Troczynski).

0272-8842/$32.00
doi:10.1016/j.ceramint.2005.09.019

calcined alumina powders (A16, ~0.5 μm, Alcoa, USA and P662B, ~3 μm, Altech, France) were used as the primary components of the composite sol. 20% diluted *ortho*-phosphoric acid (H_3PO_4, 85%, Fisher Scientific, Canada) was used for chemical bonding. Clay (Na-Bentonite, <20 nm, ADM Chemicals, USA) mixed with boehmite sol and phosphate, was used as a material for low-stiffness interface layer designed for relaxation of residual thermal stress in the coating.

Specifically, to produce the coating slurry A1, 1.5 M alumina sol (boehmite) in distilled water was combined with alumina powders (mixture of 40% A16 and 60% P662B), to give a ratio of 14–86 of sol–gel derived alumina to calcined alumina powders [7,10]. Ten percent by volume of ethyl alcohol was added into such prepared composite sol–gel solution for accelerated drying and reduction of the surface tension; the slurry was ball-milled for 24 h. The coating slurry A2 was similar but contained 100% A16 of the calcined alumina filler. The pH of alumina slurries was adjusted to 4.0 by adding 0.1 M nitric acid (HNO_3, 70%, Fishers, Canada). The initial viscosity of 40–60 cp was obtained right after completion of the ball milling, and the viscosity increased up to ~240 cp within a half hour of aging air (in preparation for coating deposition). For the clay-based porous interlayer slurry B, bentonite was combined with boehmite and water in the ratio of 1:2:20 by weight. 20% diluted mono-aluminum phosphate (MAP, $Al(H_2PO_4)_3$, PCS Purified Phosphates, USA) was added into the solution by the ratio 1:2 (weight) of MAP: water, followed by 24 h ball-milling.

The aluminum (5052 series) substrates were sand blasted using 220 Silica grit (~ 63 μm) to produce a roughness of ~9 ± 4 μm. All coating depositions were completed using commercial compressed air paint spray gun (Delta spray air spray gun, Graco Inc., USA), with ~25 psi air pressure. The estimated mass flow through the gun was ~0.08 ± 0.04 g/s, and droplet size was ~100 ± 30 of μm. To deposit the porous interlayer coating, the clay-based slurry B was sprayed first, to reach thickness of ~10 μm, the substrate located on a hot plate at ~200 °C. The flash-evaporation of the slurry particles provided 40–50 vol.% porosity of this relatively thin film layer. This film was fired at 550 °C for 30 min and slowly cooled to room temperature. Subsequently, slurry A1 was deposited on the clay interlayer, at room temperature, to achieve ~40–50 μm thick coating layer. Such coated aluminum was dried in air, and heat treated at 300 °C for 10 min 20% diluted H_3PO_4 was impregnated into the alumina-coated layer, and then the sample again fired at 300 °C for 10 min. This procedure of coating A1 slurry was repeated until the thickness of ~150 μm was reached, i.e. typically three times. Finally, slurry A2 was deposited for the total coating thickness of ~200 μm.

The effect of the compliant interlayer on reduction of thermal stresses in the coating was assessed indirectly through severe thermal shock cycling. The coated samples were heated to 300, 400 and 500 °C, maintained at the temperature for 15 min and then put into room-temperature water immediately. Three such cycles were repeated for each temperature. The amount of coating remaining on the substrate was evaluated visually and by weighing of the samples. To determine the breakdown voltage, positive ac voltage was applied to the coating surfaces using Sentry 20 ac/dc Hipot Tester (QuadTech, Inc., USA). The maximum test ranges were up to 5 kV ac and 6 kV dc, respectively. A round-shape flat-end electrode, ~3 mm diameter, made of copper, was used. The advantage of the round-shape probe over the needle like one is the increased contact area between the electrode and the surface of the coatings. Therefore, this round-shape probe significantly provides the accuracy of the breakdown voltage measurement [11]. The breakdown voltage test is also sensitive to the homogeneity of the coatings, i.e. local roughness or cracks may significantly decrease the breakdown voltage [11]. The dielectric strength (kV/mm) was calculated simply as the ratio of breakdown voltage to the coating thickness.

3. Results and discussion

The overall view of the coating structure, including the graded layers of fine particle size alumina (slurry A2) and mixture of fine and coarse particle size alumina (A1), deposited on the clay interlayer (B), is shown in Fig. 1. Fig. 2 compares the optical microscopic images of the surface of the alumina-coated aluminum with (Fig. 2b) and without (Fig. 2a) the clay interlayer. It was observed that the porous clay interlayer played an important role as a compliant buffer, to prevent formation of cracks on the coating surface. More (and longer) cracks were observed on the coating surface in Fig. 2a while not many cracks were observed in Fig. 2b. Fig. 2c shows the top view of the clay interlayer surface. We believe that the compliant interlayer has taken up most of the differential thermal strain and thus decreased thermal stress experienced by the coating [12–13]. It is expected that during processing the coatings experience both thermal up-shock (i.e. tensile stress during heat-up) and down-shock (compressive stress during cool down). This is because of the multistep processing schedule and development of chemical bonding during the heat-up process.

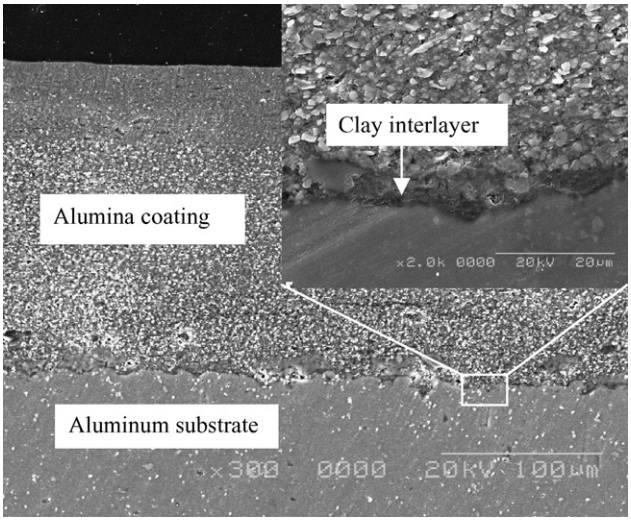

Fig. 1. SEM cross-section of the CB-CSG multilayer coating structure illustrating the porous clay interlayer.

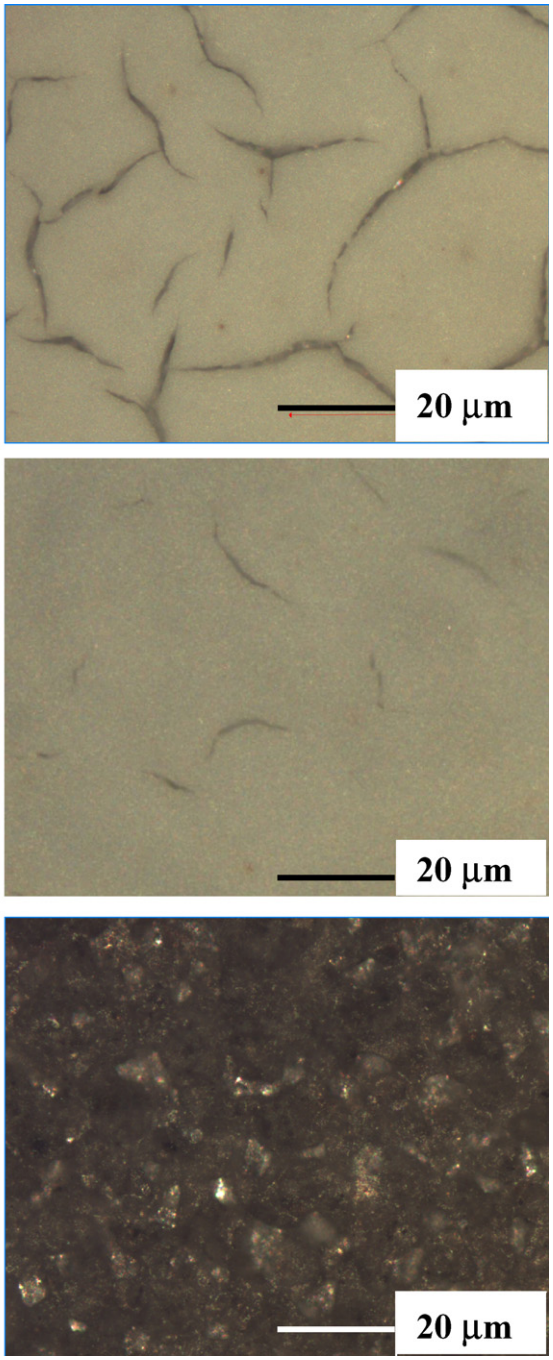

Fig. 2. Optical microscope images of the coating surfaces. CB-CSG alumina coating was either (a) directly coated on the aluminum substrate or (b) coated on the clay interlayer on the aluminum; (c) is the surface view of the clay interlayer deposited on aluminum. Thickness of alumina and clay coating layer was 20 μm and 10 μm, respectively.

As calcined clay has similar thermal expansion coefficient (5.7–8.3 × 10^{-6}/K at 20–500 °C) as alumina, majority of differential thermal expansion originated from the difference in thermal expansion coefficients of alumina and aluminum (∼8 × 10^{-6}/K versus ∼24 × 10^{-6}/K at 20–500 °C) [14]. The porosity of multilayer coating (35–40 vol.%) deposited three times from slurry A1 was similar to that of fine alumina film A2, but the pore sizes were bigger, i.e. 3–5 μm for A2 versus 1–2 μm for A1 (Fig. 3).

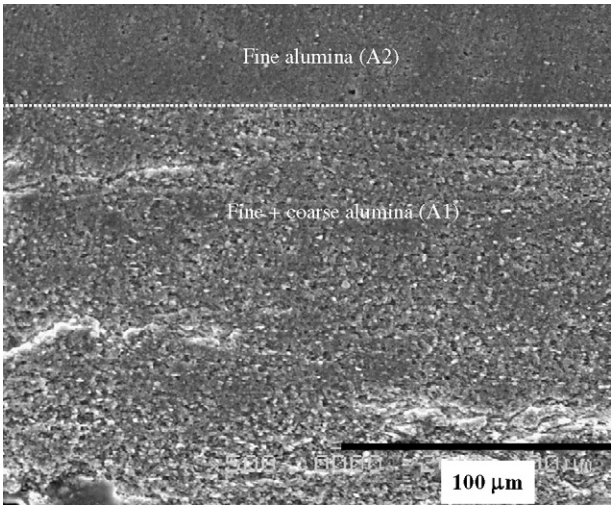

Fig. 3. Comparison of the microstructure of the top-coat (from slurry A2, 0.5 μm fine alumina) and the intermediate coatings (slurry A1, a mixture of fine 0.5 μm and coarse, ∼3 μm, alumina particles). Dots represent the border between the A1 and A2 layers.

Fig. 4 compares the results of thermal cycling of the CB-CSG alumina coatings with and without the clay-interlayer. It is observed that the coatings without clay interlayer, curve (a), started delaminating in the second quenching cycle (at 300 °C) while the coating with the clay interlayer, curve (b) survived until seventh quenching cycle, at 500 °C. Fig. 5a and b shows the result of breakdown voltage and dielectric strength, respectively. The breakdown voltage increases with the coating thickness, but the rate decreases above coating thickness of about 120 μm (Fig. 5a). Consequently, the dielectric strength reaches a maximum of about 12.3 kV/mm for the about 120 μm thick coatings (Fig. 5b). The major factors that may affect the breakdown voltage relate to microstructural features of the coating, such as porosity and cracks. It is well known that these can lead to ionization of entrapped gases in high electric fields causing locally increased current flow and thus heating. This may lead to further cracking, followed by catastrophic thermal breakdown. Due to the large difference in thermal expansion

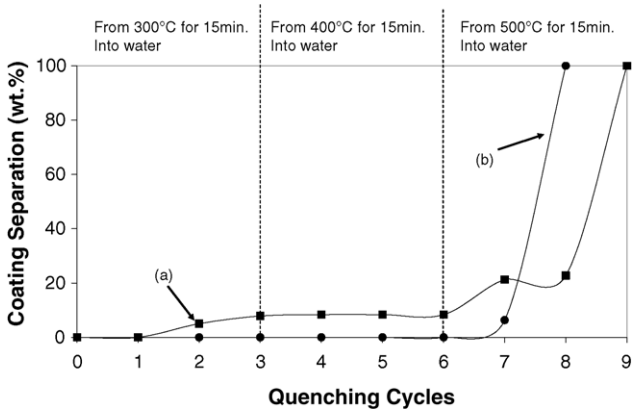

Fig. 4. Amount of CB-CSG alumina coating separation as a function of the number and temperature of the quenching cycles; (a) represents the graded alumina coatings without the clay interlayer and (b) with the clay interlayer coatings.

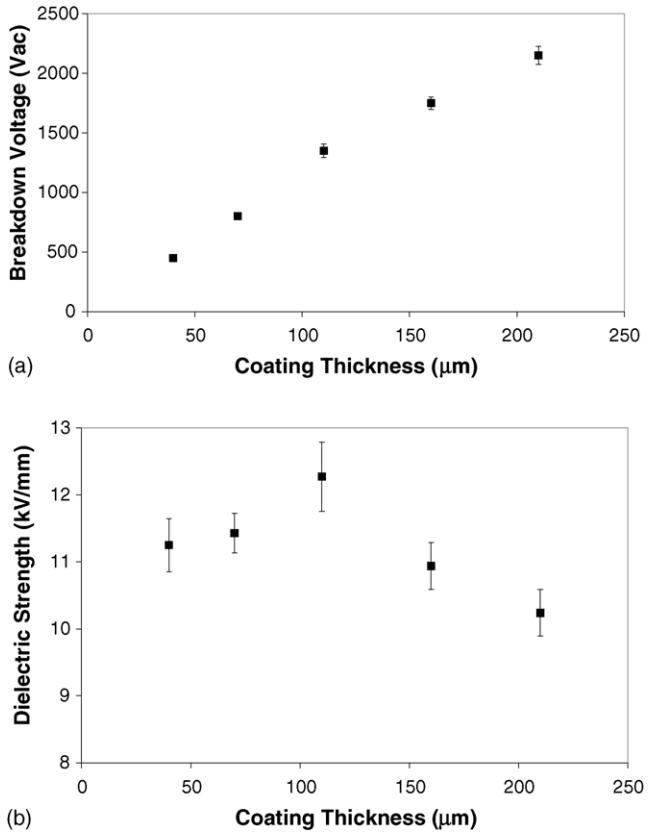

Fig. 5. Breakdown voltage (a) and dielectric strength (b) of the CB-CSG alumina-coated aluminum with compliant clay interlayer.

coefficient between the coating ($\sim 8 \times 10^{-6}$/K) and the substrate ($\sim 24 \times 10^{-6}$/K), it is to be expected that the thicker coatings experience more severe microcracking. We therefore observe that also the dielectric strength is sensitive to the thickness of the coatings. According to Fig. 5b, we expect that the coating micro-cracking intensify above 120 μm thickness, thus facilitating ionization breakdown [15]. However, the overall breakdown voltage for the coatings (Fig. 5a) increases beyond the 120 μm coating thickness, although the rate of increase with thickness is slower for the thicker coatings.

4. Conclusions

Phosphate-bonded alumina dielectric coatings, up to 200 μm thick, were successfully deposited on aluminum substrates using the low-temperature (300 °C) chemically bonded composite sol–gel technology. Two grades of average particle sizes of 0.5 μm and 3.0 μm alumina powders were used. Multilayer coating procedure was developed, including a compliant porous interlayer, to address the large thermal expansion/contraction mismatch between the alumina coating and aluminum substrate. The clay-based, porous, compliant interlayer played a key role in reducing the overall thermal shock of the coatings. Although the maximum breakdown voltage of 2100 V was reached for the thickest (200 μm) coatings, the expected ionization breakdown failure decreased dielectric strength from the maximum of 12.3 kV/mm for coatings thicker than 120 μm. It is hypothesized that the profile of dielectric strength versus coating thickness provides a reasonably good insight into the onset of coating microcracking due to excessive thermal expansion mismatch stresses in the coatings.

Acknowledgments

The authors would like to thank to the sponsors of the project, DATEC Coating Co. and the Natural Sciences and Engineering Research Council of Canada (NSERC). Help in preparation of clay interlayer samples by M. Bursa is acknowledged.

References

[1] R.W. Jones, History, in: Fundamental Principles of Sol–Gel Technology, The Institute of Metals, USA, 1989, pp. 1–4.
[2] M. Guglielmi, Sol–gel coatings on metals, J. Sol–Gel Sci. Technol. 8 (1997) 443–449.
[3] D.R. Uhlmann, G. Teowee, Sol–gel science technology: current state and future prospects, J. Sol–Gel Sci. Technol. 13 (1998) 153–162.
[4] L.L. Murrell, Sols and mixtures of sols as precursors of unique oxides, Catal. Todays 35 (1997) 225–245.
[5] T. Olding, M. Sayer, D. Barrow, Ceramic sol–gel composite coatings for electrical insulation, Thin Solid Films 581 (2001) 398–399.
[6] D.A. Barrow, M. Sayer, T.E. Petroff, Thick ceramic coatings using a sol–gel based ceramic–ceramic 0–3 composite, Surf. Coat. Technol. 76/77 (Part 1) (1995) 113–118.
[7] Q. Yang, Ph.D. thesis, Department of Metals and Materials Engineering, The University of British Columbia, 1999.
[8] T. Troczynski, Q. Yang, US Patent 6284682, 4 September 2001.
[9] R.A. Haber, P.A. Smith, Ceramics and Glasses, Engineered Materials Handbooks, vol. 4, ASM International, 1991, pp. 3–15.
[10] R.W. Grimshaw, Interpretation of particle-size analysis, in: The Chemistry and Physics of Clays, fourth ed., Western Printing Services Ltd, Bristol, 1971, pp. 395–403.
[11] J.J. O'dwyer, Part I: Theory; Chapter 1: A survey, in: The Theory of Dielectric Breakdown of Solids, Oxford University Press, 1964 pp. 1–13.
[12] R. Uribe, C. Baudin, Influence of a dispersion of aluminum titanate particles of controlled size on the thermal shock resistance of alumina, J. Am. Ceram. Soc. 86 (5) (2003) 846–850.
[13] D.J. Green, An Introduction to the Mechanical Properties of Ceramics, Cambridge University Press, 1998, pp. 94–98, 301–305.
[14] R.K. Wood, Ceramic whiteware, Ceramics and Glasses, Engineered Materials Handbooks, vol. 4, ASM International, 1991,, p. 930.
[15] R.C. Buchanan, Ceramic Materials for Electronics: Processing, Properties, and Applications, Marcel Dekker, 1986.